Chemistry of Metals and Alloys

Chem. Met. Alloys 8 (2015) 43-54
Ivan Franko National University of Lviv
www.chemetal-journal.org

On the preparation, structure and bonding of $ReSCl_3$

S.V. VOLKOV[1], V.V. SUBBOTIN[1], P.Yu. DEMCHENKO[2], R.E. GLADYSHEVSKII[2], O.G. YANKO[1]*, L.B. KHARKOVA[1]

[1] *V. Vernadsky Institute of General and Inorganic Chemistry, National Academy of Sciences of Ukraine, Palladin Ave. 32/34, UA-03680 Kyiv, Ukraine*
[2] *Department of Inorganic Chemistry, Ivan Franko National University of Lviv, Kyryla i Mefodiya St. 6, UA-79005 Lviv, Ukraine*
** Corresponding author. E-mail: oleg_yanko@mail.ru*

Received May 25, 2015; accepted June 24, 2015; available on-line September 1, 2015

The reaction of Re_2O_7 with a solution of S in S_2Cl_2 at 100°C produced rhenium sulfur trichloride, $ReSCl_3$. The compound was found to have a polymeric linear structure $[\{ReCl_2(\mu\text{-}Cl)\}_2(\mu\text{-}S)_2]_\infty$, which represents a new structure type (space group *C*2/*m*, *a* = 11.4950(7), *b* = 6.5626(3), *c* = 5.9938(4) Å, *β* = 95.199(4)°, *Z* = 4). The structure is closely related to the $NbCl_4$-type and expands the series of similar one-dimensional chain structures. Distorted $Re[Cl_4S_2]$ octahedra share edges to form infinite straight chains along the [010] direction and the Re atoms are arranged in pairs with alternatively short (2.965 Å) and long (3.598 Å) Re–Re distances. Electronic structure calculations and chemical bonding analysis, using the electron density/electron-localizability indicator (ELI) approach, indicated overall metallic character and revealed a combination of covalent polar Re–Cl and Re–S bonds and weak Re–Re non-polar metallic bonds, yielding the ELI-based oxidation numbers (ELIBON) $Re^{+3.40}S^{-1.20}[Cl1^{-0.68}]_2Cl2^{-0.84}$.

Rhenium sulfidochlorides / Crystal structure / One-dimensional chain structures / Density functional calculations / Electron localizability indicator / Chemical bonding

Introduction

Syntheses of rhenium chalcogenido-halides in systems containing rhenium, sulfur and chlorine have led to the formation of 14 rhenium sulfidochlorides, which are simple, coordination or cluster compounds. Most of them have been obtained by solid-state synthesis, and only for five of them a complete crystal structure determination has been performed (Table 1).

For instance, sulfidochlorides of the composition $ReSCl_2$ [1,2], $ReSCl_4$ [1], $ReS_3Cl{\cdot}S_2Cl_2$ [1], and $Re_2S_3Cl_4$ [1] have been obtained by the interaction of the cluster trirhenium nonachloride and rhenium pentachloride with sulfur in a wide temperature range and in a wide range of molar ratios of the constituents. It can be pointed out as a general rule that an increase of the temperature (125-240°C) results in the substitution of an increasing number of sulfur atoms for chlorine. The ratio of the reagents does in general not affect the composition of the reaction product. Unfortunately, it is not always possible to predict the composition. Therefore, the ratio of the reagents was generally chosen arbitrarily, using a large excess of the reagent that can easily be removed after the synthesis.

By allowing ReS_2 or Re_2S_7 and chlorine to react at different temperatures, $ReSCl_2$ and $Re_2S_3Cl_4$ were formed [3,4] by breaking of Re–S bonds and formation of Re–Cl bonds. Sulfur chlorides were formed as by-products. Rhenium(VII) sulfide begins to interact with chlorine at 120°C, whereas rhenium(IV) sulfide does so at considerably higher temperatures (400-450°C). Chlorination of $Re_2S_3Cl_4$ at 400-450°C also yields $ReSCl_2$ [3].

A distinctive feature of the interaction of metallic rhenium with its pentachloride and sulfur is the relatively low reaction rate, which is controlled by diffusion in the solid state. $Re_6S_4Cl_{10}$ and $Re_6S_5Cl_8$, which belong to a series with the general formula $Re_6S_{4+q}Cl_{10-2q}$ (where q = 0-4), have been obtained by controlled heating of finely ground, blended and pressed mixtures in evacuated silica tubes at 450-825°C. The composition of the reaction products is mainly determined by the ratio of the constituents [11]. The reaction of rhenium with sulfur and chlorine at 1060-1100°C led to the formation of $Re_6S_8Cl_2$, belonging to the same series [12]. Varying the ratio of the starting substances, other rhenium sulfidochlorides of this series can probably be synthesized as well. This means that syntheses of this kind are fully predictable

Table 1 Preparation methods used for known rhenium sulfidochlorides.

No.	Compound	Preparation method, conditions	Reference
1	$ReSCl_2$	$2ReCl_5 + 4S$, 160-270°C	[1]
		$Re_3Cl_9 + S$	[2]
		$Re_2S_7 + Cl_2$, 400-450°C	[3]
		$ReS_2 + Cl_2$, 400-450°C	[3,4]
		$Re_2S_3Cl_4 + Cl_2$, 400-450°C	[3]
2	$ReSCl_3$	$ReCl_5 + Sb_2S_3$, in CS_2 at 20°C	[5]
		$ReCl_5 + S_2Cl_2$, 140°C	[6]
3	$ReSCl_4$	$ReCl_5 + S$, 125°C	[1]
		$Re_3Cl_9 + S_2Cl_2$, DTA	[1]
4	$ReS_3Cl{\cdot}S_2Cl_2$	$2ReCl_5 + 8S$, 220°C	[1]
		$2ReCl_5 + 9S$, 240°C	[1]
		$ReCl_5 + 7S$, 200°C	[1]
		$ReS_2 + S_2Cl_2$, DTA	[1]
5	$Re_2S_3Cl_4$	$2ReCl_5 + 4S$, 125-160°C	[1]
		$2ReCl_5 + 9S$, 180°C	[1]
		$Re_2S_7 + Cl_2/CO_2$ (1:5), 120°C	[3]
6	ReS_2Cl_3	$ReCl_5 + S_2Cl_2$, 300°C	[6]
7	$ReCl_5(SCl_2)_4$	$ReCl_5 + SCl_2$, 20-100°C	[6]
8	Re_2SCl_{12} [a]	$ReCl_5 + S_2Cl_2$, 20°C	[7]
		$Re + SCl_2$, 400°C	[8]
9	$Re_2S_4Cl_7$	$ReCl_5 + S + S_2Cl_2$, 20-100°C	[7]
		$ReCl_5 + S_2Cl_2$, in CS_2 at 20°C	[7]
10	$Re_3S_4Cl_8$	$Re_2S_4Cl_7 + S_2Cl_2$, 250°C	[7]
11	$Re_3S_7Cl_7$ [b]	$ReOCl_4 + S + S_2Cl_2$, 200°C	[9]
		$Re_2O_7 + S + S_2Cl_2$, 200°C	[7]
		$ReCl_4 + S + S_2Cl_2$, 130°C	[10]
12	$Re_6S_4Cl_{10}$ [c]	$ReCl_5 + Re + S$, 450-825°C	[11]
13	$Re_6S_5Cl_8$ [d]	$ReCl_5 + Re + S$, 450-825°C	[11]
14	$Re_6S_8Cl_2$ [e]	$Re + S + Cl_2$, 1060-1100°C	[12]

Crystallographic data:
[a] $SCl_3[Re_2Cl_9]$: monoclinic, $P2_1/m$, a = 8.341(4), b = 10.533(5), c = 8.661(4) Å, β = 91.90(4)°, Z = 2 [8].
[b] $Re_3S_7Cl_7$: trigonal, $P3$, a = 8.999(3), c = 22.516(5) Å, Z = 4 [9], and trigonal, $P31c$, a = 8.9983(3), c = 22.493(2) Å, Z = 4 [10].
[c] $Re_6S_4Cl_{10}$: triclinic, P-1, a = 8.910(2), b = 12.441(2), c = 8.842(1) Å, α = 95.79(1), β = 97.61(1), γ = 83.68(1)°, Z = 2 [11].
[d] $Re_6S_5Cl_8$: triclinic, P-1, a = 9.050(3), b = 13.045(4), c = 8.767(4) Å, α = 96.08(4), β = 116.08(3), γ = 80.50(3)°, Z = 2 [11].
[e] $Re_6S_8Cl_2$: monoclinic, $P2_1/n$, a = 6.364(1), b = 11.304(2), c = 9.914(2) Å, β = 100.40(1)°, Z = 2 [12].

as to the end product. The compounds forming in the above systems contain rhenium in the low oxidation state +3 and are hexanuclear cluster sulfidochlorides $[Re_6(\mu_3\text{-}S)_{8-q}(\mu_3\text{-}Cl)_q]Cl_{q+2}$ (where q = 0-4) [11,12]. This explains their high thermal and chemical stability. The main disadvantages of heterogeneous synthesis are the diffusion barriers, which limit the rate of the processes, and often the impossibility to obtain high-purity homogeneous products. An advantage of the same methods is that the possibility to carry out the synthesis at ~1000°C allows obtaining cluster structures that do not form at low temperatures.

Non-aqueous solvents such as sulfur chlorides and carbon disulfide have been used as reaction media for the synthesis of rhenium sulfidochlorides in liquid media. Liquid sulfur chlorides usually act as solvents and starting reagents at the same time. Rhenium pentachloride gives the adduct $ReCl_5{\cdot}4SCl_2$ in sulfur dichloride at 20-100°C [6], while in sulfur monochloride $ReSCl_3$ [6], ReS_2Cl_3 [6] and Re_2SCl_{12} [7] are observed at different temperatures. According to the authors' assumption, the first two compounds are polymers. The last compound, which has also been obtained by the interaction of metallic rhenium with sulfur dichloride at 400°C [8], is an ionic complex $(SCl_3)^+[Re_2Cl_9]^-$. Re_3Cl_9 interacts with S_2Cl_2 to form $ReSCl_4$ [1], while ReS_2 forms $ReS_3Cl{\cdot}S_2Cl_2$ [1]. Solution of sulfur in S_2Cl_2 with $ReCl_5$ produces $Re_2S_4Cl_7$ [7], while with rhenium(VI) oxychloride [9], rhenium(VII) oxide [7] and rhenium(IV) chloride [8], a trinuclear cluster $Re_3S_7Cl_7$ of the structure

$[Re_3(\mu_3\text{-}S)(\mu\text{-}S_2)_3Cl_6]^+Cl^-$ was observed. In carbon disulfide, $ReSCl_3$ [5] is formed from the starting compound $ReCl_5$ in the presence of Sb_2S_3, and $Re_2S_4Cl_7$ [7] in the presence of S_2Cl_2, with subsequent transformation into the trinuclear complex $Re_3S_4Cl_8$ [7] at 250°C.

In contrast to the heterophase synthesis, the liquid-phase method is limited by the temperature due to the decomposition of the sulfur chlorides and the production of excess pressure, since the synthesis is usually carried out in a closed system. A salient feature and the main advantage of synthesis in liquid media is the homogenization stage (even short-term), when the starting substances completely dissolve in the solvent, which is often a starting reagent at the same time. The liquid-phase synthesis method ensures: i) a relatively high reaction rate, due to the good contact between the reactants and the high diffusion rate in the liquid; ii) a high degree of purity and homogeneity of the reaction products thanks to crystallization from the liquid; iii) the possibility of growing more or less large crystals from the solutions, which is convenient for the investigation of the compounds; and iv) relative simplicity and safety.

The compound $ReSCl_3$ has been obtained in liquid media. Rhenium pentachloride reacts with diantimony trisulfide in a carbon disulfide medium at room temperature by the reaction $3ReCl_5 + Sb_2S_3 = 3ReSCl_3 + 2SbCl_3$ [5]. The interaction of rhenium(V) chloride with sulfur monochloride under long boiling in an argon stream at 140°C, according to the reaction $ReCl_5 + 2S_2Cl_2 = ReSCl_3 + 3SCl_2$, yielded $ReSCl_3$ in the form of black microcrystals [6]. This paper deals with the synthesis of $ReSCl_3$ (**I**) from the interaction between rhenium(VII) oxide and a solution of sulfur in sulfur monochloride at 100°C, and with the investigation of its crystal structure and chemical bonding.

Experimental

Synthesis

The synthesis of **I** was carried out in an L-shaped glass reactor. A solution of S in S_2Cl_2 (5 ml, 20 %) was added to Re_2O_7 (1 g). Upon moderate heating (40-50°C) Re_2O_7 completely dissolved in the reaction medium. The exothermic reaction was accompanied by release of gaseous SO_2. The reaction mixture was heated in a moisture-protected open reactor to complete isolation of SO_2 at 80-90°C for 120 h. After sealing, the reactor was heated at 100°C for 180 h. The resulting solid product was separated from the liquid phase by decantation. Then the part of the reactor containing the liquid was frozen in liquid nitrogen in order to avoid explosion of the reactor during opening. The solid product was transferred to a Schlenk filter, filtered under a flow of inert gas, washed with S_2Cl_2 and CCl_4, and dried under vacuum. A brownish-black microcrystalline powder (1.1 g, 82 % yield) was obtained, which rapidly decomposes in air.

Characterization

Elemental analysis was performed on an ElvaX Light X-ray fluorescence spectrometer. Results (%) for **I**: calc. Re, 57.36; S, 9.88; Cl, 32.76; found Re, 57.16; S, 9.74; Cl, 33.10. The bulk homogeneity of the product was confirmed by scanning electron microscopy (SEM), using of a REMMA-102-02 microscope, and by X-ray powder diffraction (XRPD), collecting data on a STOE STADI P diffractometer. Raman spectra were measured in reflection geometry at room temperature, using a Horiba Jobin-Yvon T-64000 Raman spectrometer equipped with a cooled CCD detector. An Ar–Kr ion laser line with a wavelength of 514.5 nm, focused on the sample to a spot of ~1 μm diameter at a radiation power of about 0.1 mW, was used for excitation.

X-ray crystal structure determination

XRPD data for the solution and refinement of the crystal structure were collected in the transmission mode on a STOE STADI P diffractometer [13] with the following setup: Cu$K\alpha_1$-radiation, curved Ge (111) monochromator on the primary beam, $2\theta/\omega$-scan, angular range for data collection 6.000-89.985 °2θ with increment 0.015 °2θ, linear position-sensitive detector with step of recording 0.480 °2θ and time per step 120 s, $U = 40$ kV, $I = 40$ mA, $T = 24$°C. A calibration procedure was performed utilizing NIST SRM 640b (Si) [14] and NIST SRM 676 (Al_2O_3) [15] standards. Analytical indexing of the powder pattern and determination of the space group were performed using N-TREOR09 [16]. The crystal structure was solved by direct methods, using EXPO2014 [17], and was refined by the Rietveld method [18] with the program FullProf.2k (version 5.40) [19,20], applying a normalized Pearson VII profile function and isotropic approximation for the atomic displacement parameters. An absorption correction was considered by measuring the absorption factor for a sample transmission foil [13] and applied during the Rietveld refinement according to the type "Transmission geometry (STOE)" [19,20]. The crystallographic data were standardized with the program STRUCTURE TIDY [21] and the program DIAMOND [22] was used for structural visualization.

*Crystal data for **I***

Cl_3ReS, $[\{ReCl_2(\mu\text{-}Cl)\}_2(\mu\text{-}S)_2]_\infty$, rhenium sulfur trichloride, $M = 324.62$ g mol^{-1}, monoclinic, space group $C2/m$ (no. 12), $a = 11.4950(7)$, $b = 6.5626(3)$, $c = 5.9938(4)$ Å, $\beta = 95.199(4)$°, $V = 450.29(5)$ Å^3; $Z = 4$; $\rho_{calc} = 4.788$ g cm^{-3}, μ(Cu$K\alpha$) = 71.854 mm^{-1}; 222 reflections measured, 24 parameters refined, reliability factors $R_I = 0.0402$, $R_F = 0.0345$, $R_p = 0.0781$, $R_{wp} = 0.104$, $R_{exp} = 0.0976$, $\chi^2 = 1.13$. Further details of the crystal structure investigation are available as supporting material (cif file).

Quantum-chemical calculations

Density Functional Theory (DFT) electronic structure calculations were carried out for **I** using the experimental structural parameters determined above and the all-electron full-potential linearized augmented-plane wave code Elk [23], with PBEsol [24] generalized gradient approximation. Relativistic effects were taken into account by employing the fully relativistic mode for the core states and by using a scalar relativistic approximation [25] with spin-orbit coupling for the valence states. The valence-basis sets were set by default as provided by the code. The total energy values converged with an accuracy of ~3 meV for the 10×10×10 (504 points) *k*-point mesh in the Brillouin zone. Plane waves were included up to a cutoff energy of 238 eV; electronic states were occupied with a Fermi-Dirac smearing width of 0.027 eV. Real-space chemical bonding in **I** was characterized by combining topological analyses of the electron density (ρ) according to the quantum theory of atoms in molecules (QTAIM) proposed by Bader [26] and the electron localizability indicator (ELI), which was evaluated in the ELI-D representation [27-29]. Electron density and ELI-D were calculated on an equidistant grid with a mesh of 0.05 a_0. The purpose of the topological analysis was to find the attractors and basins of attractors and the electron populations of the basins and their intersections, by integration of the electron density in QTAIM/ELI-D basins. The calculations were carried out by the program DGrid 4.6e with Elk support [30,31] and the VESTA [32] and ParaView program packages [33] were used for visualization.

Results and discussion

Sulfidotrichloridorhenium(V) $ReSCl_3$ (**I**) was obtained at 100°C as an air-sensitive, brownish-black, microcrystalline powder with metallic luster (Fig. 1), according to the scheme:

$$2Re_2O_7 + 6S_2Cl_2 \rightarrow 4ReSCl_3\downarrow + 7SO_2\uparrow + S.$$

Fig. 2 shows a Raman spectrum of **I**. The weak lines at 312, 317 and 325 cm^{-1} were assigned to stretching vibrations of the Re–Cl bonds [34] and the lines at 110_w, 126_s, 143_m, 169_s, and 199_s cm^{-1} (with weak overtone lines at 255, 285, and 401 cm^{-1}) to deformation vibrations of Cl–Re–Cl bonds [35]. The weak lines at 230, 270, and 278 cm^{-1} relate to deformation vibrations of S–Re–S bonds, while the lines 359_s, 378_w, 387_w, 415_w, 444_w, and 463_s cm^{-1} were assigned to stretching vibrations of the Re–S bonds [34]. By combining proposed correlations [35] between experimental frequencies and force constants for metal-metal bonds with empirical relations [36,37] between the bond lengths and force constants, the value $\nu = 111.9$ cm^{-1} for weak Re–Re bonding interaction was calculated, which can be associated with the weak experimental line at 113 cm^{-1}.

Although at least fourteen rhenium sulfidochlorides have been reported up to now (Table 1), structural evidence based on single-crystal XRD data exists only for five of them. For the other compounds sometimes only the preparation of the species has been reported, in some cases together with chemical analysis and primary characterization by spectroscopic methods, differential thermal analysis (DTA) and qualitative analysis from XRPD data.

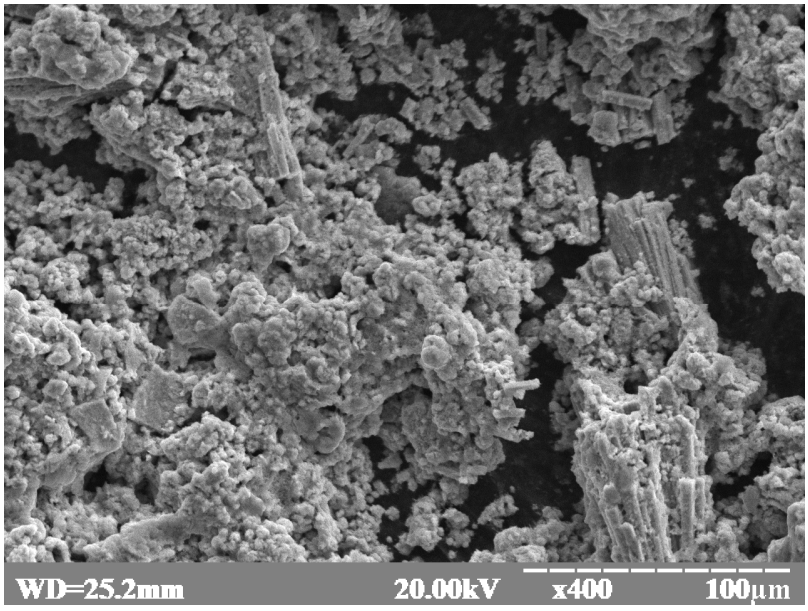

Fig. 1 SEM image of the reaction product.

The reasons were in inhomogeneous products, the instability of the compounds, and the lack of suitable single crystals for structural investigations. The latter problem can in many cases be successfully solved by using XRPD data for crystal structure solution and refinement [38]. As an example for chalcogenido-halogenides of transition metals, one can mention the nonaselenium ring found by XRPD in $Rh_2Se_9Cl_6$ [39], then confirmed by single-crystal XRD in $Ir_2Se_9Cl_6$ [40]. Since attempts to obtain single crystals suitable for single-crystal XRD failed, XRPD data (Fig. 3) were used for the structural investigation of **I**.

The structure of **I** (Table 2, Fig. 4) belongs to the family of one-dimensional chain structures and is close related to the structure type $NbCl_4$ [41-44]. Both structures are built up of close-packed Cl (Cl/S) layers in hexagonal stacking, with Nb (Re) atoms occupying 1/4 of the octahedral voids. In **I** distorted $Re[Cl_4S_2]$ octahedra share edges to form infinite straight chains along the [010] direction and the Re atoms are arranged in pairs with alternating short and long Re–Re distances. The long rhenium–rhenium distance is 3.598 Å, while the short distance is 2.965 Å (Table 2, Fig. 5(b)) and a comparison with the interatomic distance of 2.74 Å in metallic rhenium suggests the presence of weak metal–metal interactions. So-called α-$ReCl_4$ [47] was found to crystallize in the $NbCl_4$ structure type, however, without refinement of the atomic coordinates. Assuming the atomic coordinates refined for $NbCl_4$ [46], the Re–Re distances are 2.886 and 3.615 Å. The Re–Cl distances in **I** are practically the same for the terminal axial chlorine atoms (2.289 Å) and the bridging chlorine atoms (2.274 Å), and the mean distance is in good agreement with typical Re–Cl^- interatomic distances (2.316 Å [48]). The 2.436 Å long bond between rhenium and the bridging sulfur atoms is longer than the typical Re–S interatomic distance given as 2.334 Å in [48], but is close to the sum of the effective ionic radii of Re and S with formal charges +5 and –2, respectively: r(Re)+r(S) = 2.42 Å [49].

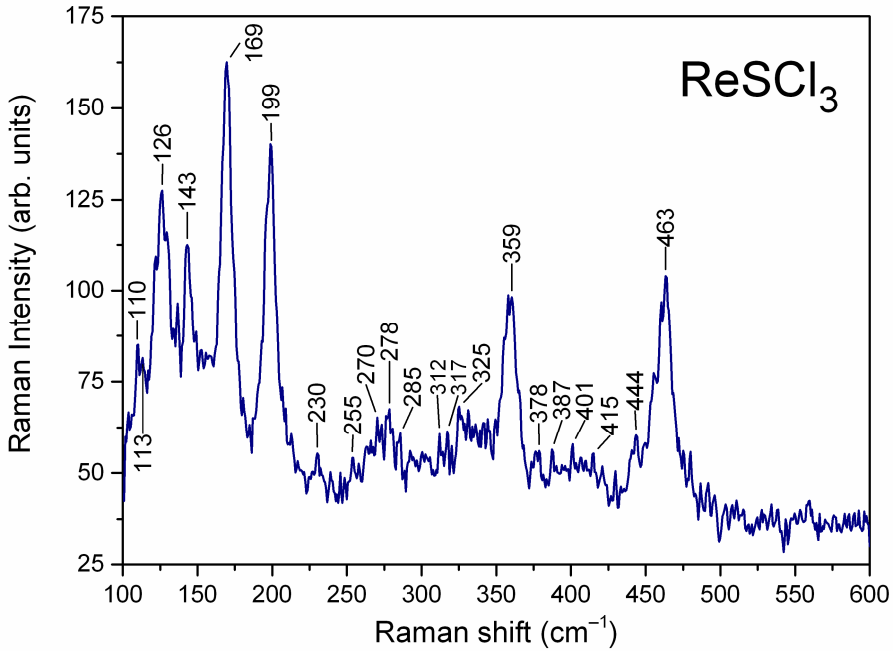

Fig. 2 Raman spectrum of **I**.

Table 2 Fractional atomic coordinates and isotropic displacement parameters for **I**.

Site	Wyckoff position	x	y	z	B_{iso} (Å^2)
Re	4*g*	0	0.2259(6)	0	0.62(8)
S	4*i*	0.3858(19)	0	0.146(3)	1.1(6)
Cl1	8*j*	0.1286(6)	0.242(2)	0.3143(13)	1.3(3)
Cl2	4*i*	0.1115(17)	0	0.826(3)	1.2(6)
Interatomic distances (in Å)					
Re – Re [1]		2.965(6)	Re – 2Cl1		2.289(7)
Re – Re [2]		3.598(6)	Re – 2S		2.436(15)
Re – 2Cl2		2.274(15)			

[1] –*x*, –*y*, –*z*, [2] –*x*, 1–*y*, –*z*

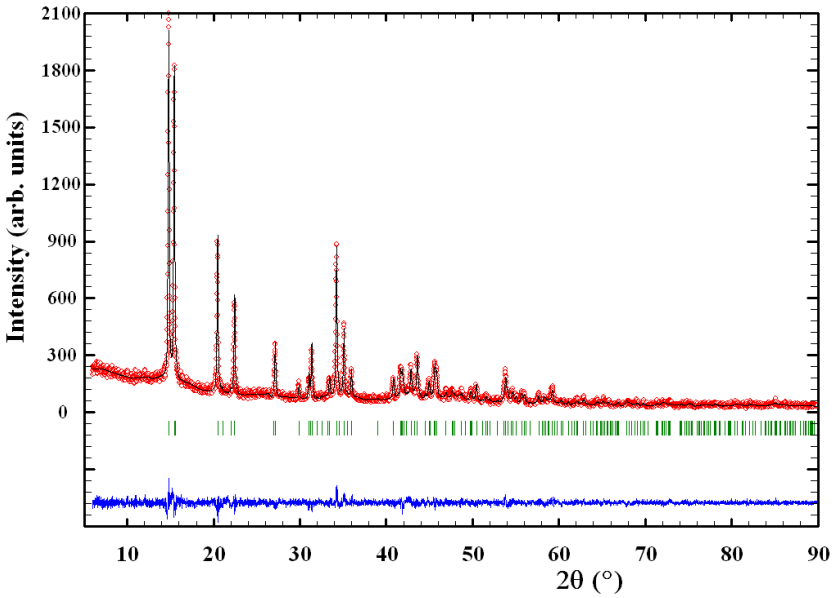

Fig. 3 Observed and calculated XRPD patterns for **I** (Cu*K*α_1-radiation). Experimental data (circles) and calculated profile (solid line through the circles) are presented together with the calculated Bragg positions (vertical ticks) and difference curve (bottom solid line).

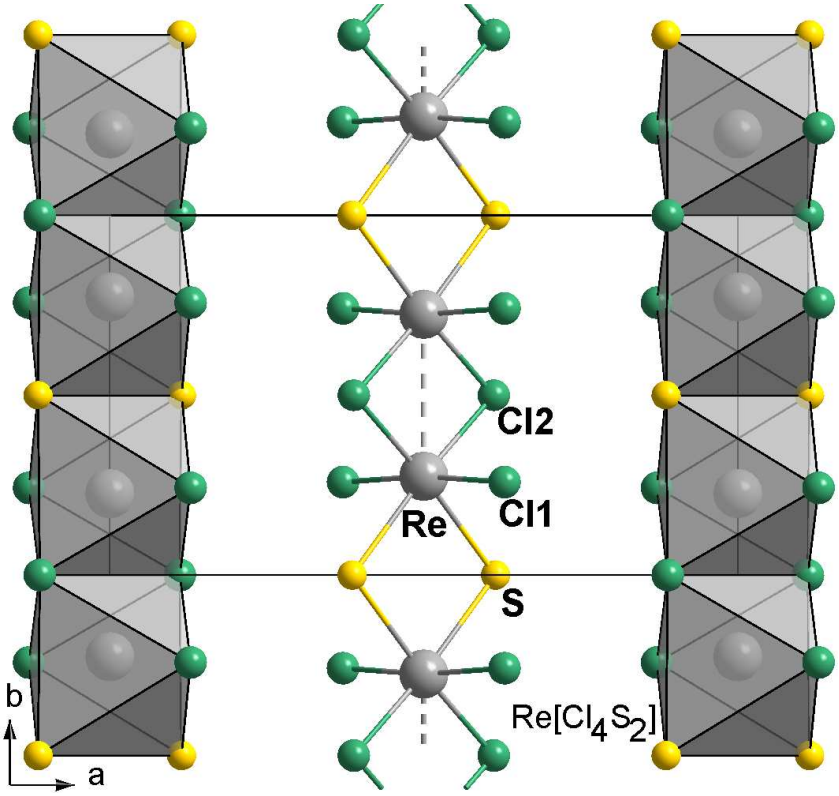

Fig. 4 A view of the crystal structure of **I** along the *c* axis.

The structure of **I** is polymeric with infinite linear chains $[\{ReCl_2(\mu\text{-}Cl)\}_2(\mu\text{-}S)_2]_\infty$. The formation of infinite linear or zigzag chains, with or without metal–metal bonding, is typical for transition metal tetrachlorides. Five different structure types ($TcCl_4$, $NbCl_4$, β-$MoCl_4$, β-$ReCl_4$, and $OsCl_4$) have been

assigned to second- and third-row transition metal tetrachlorides [50]. Based on data in the database Pearson's Crystal Data [46], we identified four structure types formed by second- and third-row transition metal chalcogen-halogenides with the following restrictions: i) only binuclear clusters with pronounced or weak metal-metal interactions; ii) infinite one-dimensional linear or zigzag chains; and iii) neutral chains (*i.e.* charged chains, such as those observed in ruthenium/rhodium tellurochlorides [51] or $Ta_3Se_8Br_6$ [52] have not been considered). These structure types are $NbSeBr_3$ [53], $NbSeI_3$ [54], $Nb_3Se_5Cl_7$ [55], and MoS_2Cl_3 [56]. The new $ReSCl_3$ structure type expands this family (Fig. 5).

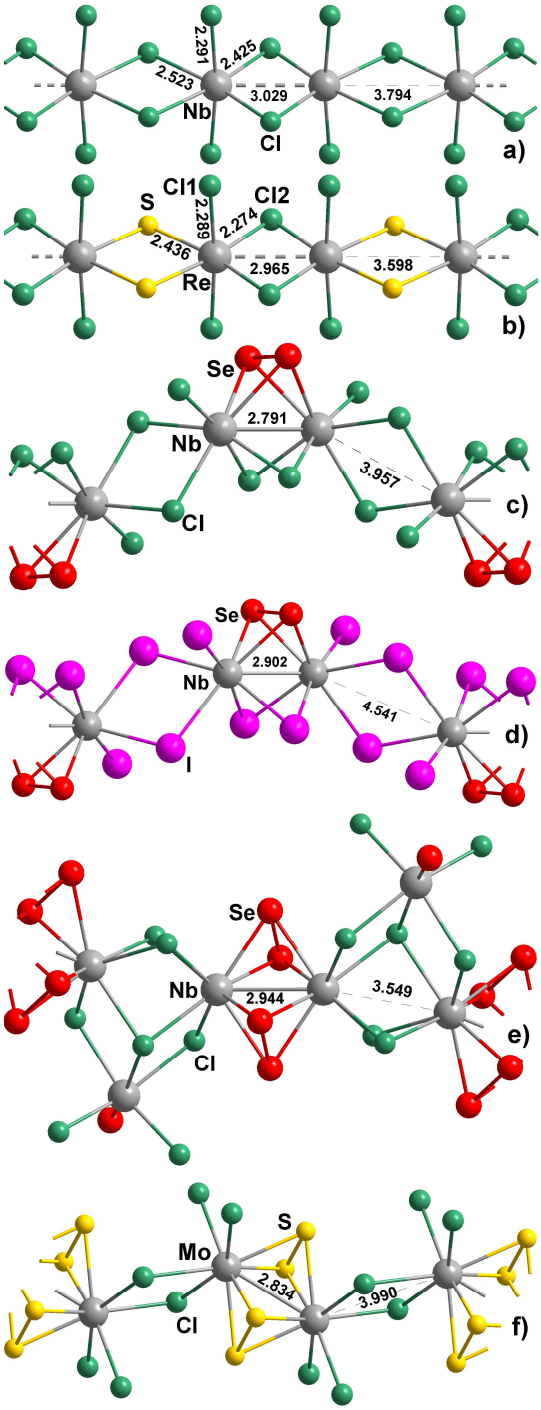

Fig. 5 Structure types for second- and third-row transition-metal chalcogen-halogenides containing neutral infinite chains. a) $NbCl_4$ (to compare with **I**): *C*2/*m*, a = 11.823, b = 6.823, c = 8.140 Å, β = 131.56° [41]. b) $ReSCl_3$: *C*2/*m*, a = 11.4950, b = 6.5626, c = 5.9938 Å, β = 95.199°. c) $NbSeBr_3$: data for $NbSeCl_3$: *P*2/*c*, a = 6.2993, b = 6.7205, c = 11.962 Å, β = 98.71° [45]. d) $NbSeI_3$: *C*2/*c*, a = 7.110, b = 13.899, c = 13.688 Å, β = 99.58°. e) $Nb_3Se_5Cl_7$: $P2_1/m$, a = 7.599, b = 12.675, c = 8.051 Å, β = 106.27°. f) MoS_2Cl_3: $P2_1/c$, a = 6.168, b = 7.244, c = 13.345 Å, β = 116.17°. The crystallographic data have been standardized [21,46].

In order to study the relationship between the crystal and electronic structures, firstly the electronic density of states (DOS) was calculated. Fig. 6 presents the total DOS and partial DOS of the Re 5*d*, S and Cl 3*p* states, which are by far the dominant states in the energy range shown on the figure. The DOS calculations indicate metallic character. The valence and conduction peaks near the Fermi level (E_F) are dominated by Re 5*d* orbitals, hybridized with 3*p* orbitals from chlorine and sulfur atoms, while the peaks at the bottom of the valence band mainly show 3*p*-orbital contributions. From the DOS at E_F, $N(E_F)$ = 1.22 states/(eV primitive cell), we can extract the Sommerfeld electronic heat capacity coefficient, γ= 1.44 mJ/K^2 mol Re, which is close to the value of 2.3 mJ/K^2 mol for pure rhenium. It may be noted that the DOS plots, obtained by the LSDA+*U* approach with an effective Coulomb repulsion potential *U* = 2.8 eV for Re 5*d* electrons, are almost identical in the vicinity of the E_F to those described above, but $N(E_F)$ = 0.74 states/(eV primitive cell) is somewhat lower.

Considering the constituent elements in **I** and related compounds, similar metallic characteristics have been found, *e.g.* for all technetium tetrahalides [57] and for the hypothetical undistorted structures of TcS_2, ReS_2 and $ReSe_2$ [58]. ReS_2, which crystallizes with a distorted 1T crystal structure, is a direct-bandgap semiconductor [58,59], but Cl-doping leads to a shift of the Fermi level to the bottom of the conduction band, which suggests n-type doping [60]. For ReS_2 with a hypothetical undistorted 3R structure ($CdCl_2$ type) and Re–Re distances of 3.20 Å (*i.e.* without metal–metal bonding) it was concluded [58] that the high DOS at the Fermi level, in combination with electron-phonon interaction, explains the instability of this structure. The formation of Re–Re bonds lowers the total energy of the system and the stable distorted 1T structure exhibits semiconductor characteristics [59]. Consequently, we can suggest that the structure of **I** with relatively high DOS at E_F, but with weak metal–metal interaction, is on the stability boundary.

At the next step, the real-space chemical bonding in **I** was characterized. Integration of the electron density over QTAIM (quantum theory of atoms in molecules, proposed by Bader [26]) basins gave the following electron populations: Re: 73.45 *e*, S: 16.41 *e*, Cl1: 17.39 *e*, Cl2: 17.36 *e*; and the effective atomic charges $Re^{+1.55}S^{-0.41}(Cl1^{-0.39})_2Cl2^{-0.36}$. The distribution of the electron localizability indicator (ELI-D, ϒ) [27-29] along the chain (Fig. 7) reveals pronounced spherical envelopes of high ELI-D around the more electronegative S and Cl atoms, visualizing polarization of the electron density between sulfur/chlorine and rhenium towards the S/Cl atoms. Increased values of ELI-D are clearly seen between the rhenium pairs with short Re–Re distance, confirming the presence of weak metal–metal interactions.

Quantitative data for the chemical bonding in **I** from the topological analysis are presented in Table 3 and on Fig. 8. Integration of the electron density over ELI-D basins and subtraction of the electron numbers for neutral atoms allows obtaining the so-called balance of the ELI-based oxidation numbers (ELIBON) [61]: $Re^{+3.40}S^{-1.20}[Cl1^{-0.68}]_2Cl2^{-0.84}$. The Re–S and Re–Cl bonds are polar covalent bonds, as

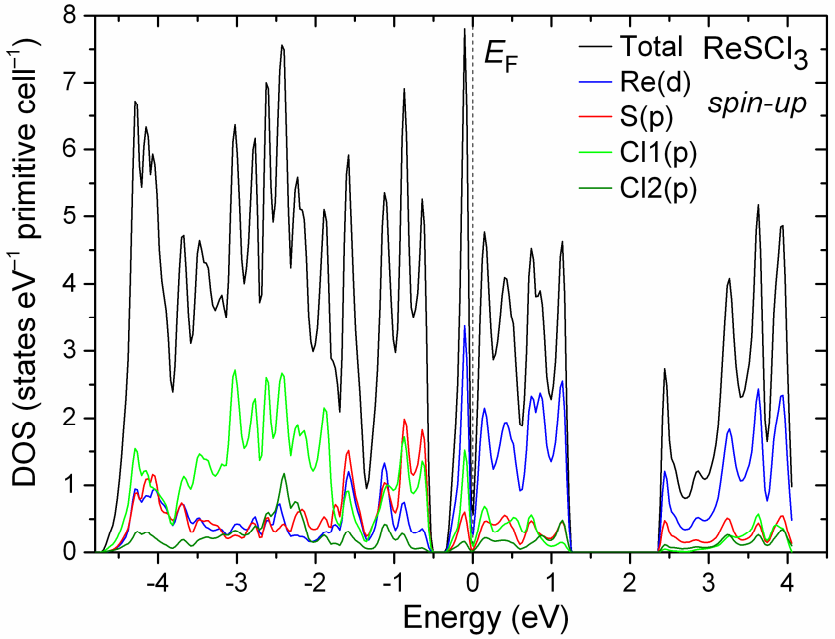

Fig. 6 Total and orbital-projected DOS of **I** for a primitive unit cell (10 atoms). The Fermi energy E_F was set to zero. Since the DOS in majority and minority spins are symmetrical, DOS curves are shown for the spin-up channel only.

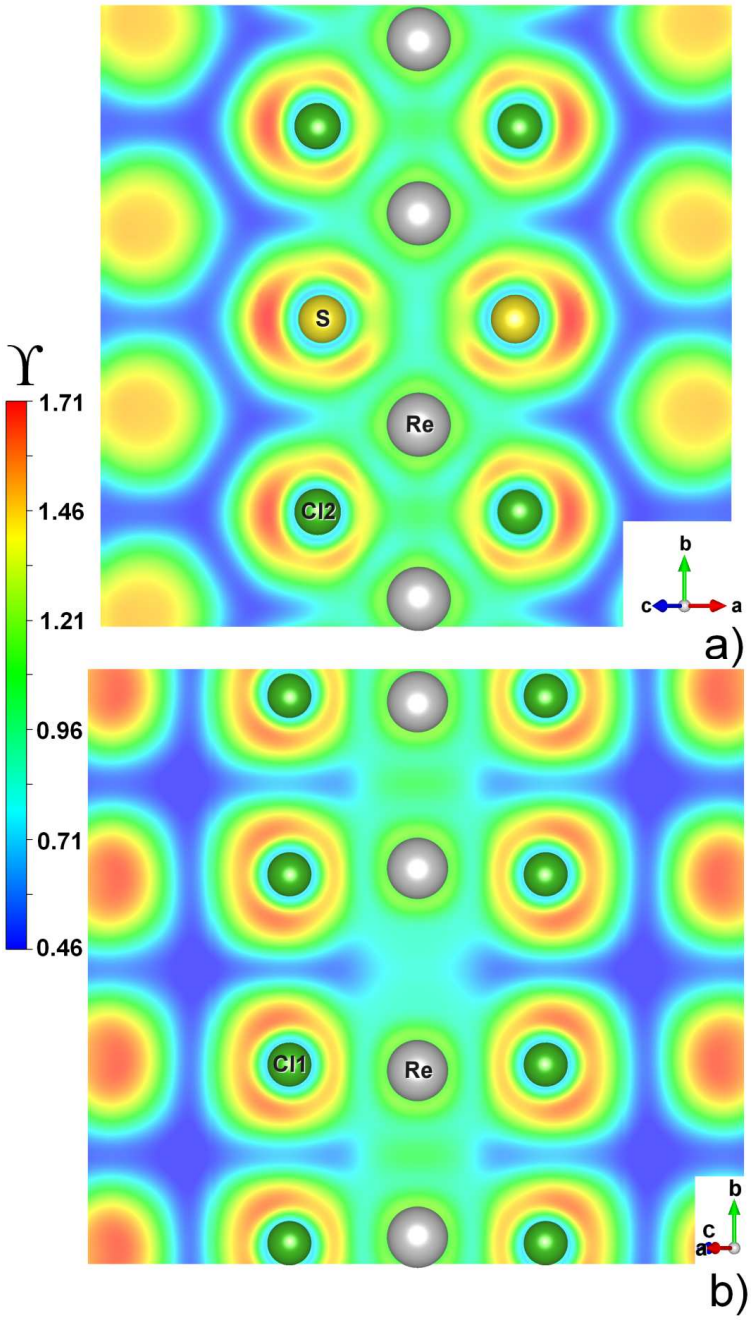

Fig. 7 Electron localizability indicator (ELI-D, ϒ) in **I**. ELI-D distribution in the lattice planes of: a) Re–S–Re and Re–Cl2–Re bridges; b) Re–Cl1.

indicated by the value of about 0.6 of the bond polarity index [62], whereas the weak Re–Re bond (0.206 *e* per Re) is non-polar. While the Re–S bond has the character of a nearly single bond formed by an average of 0.9 bonding electron pairs, which are polarized towards the S atom with a polarity of 0.57, the character of the Re–Cl1 bond is close to ionic: only 0.455 bonding electron pairs form a partial single bond, and the two monosynaptic basins (lone pairs) have an enlarged population (6.7 *e*). Although the bridging Cl2 atom has an almost filled third shell (17.84 *e*), the character of the two Cl2–Re bonds is strongly polar covalent: two 0.53 bonding electron pairs form two partial single bonds, which are strongly polarized towards the Cl2 atom with a polarity of 0.64.

The interaction between the chains in **I** due to dispersion forces is shown on the example of the bridging Cl2 and S atoms (Fig. 8b). The ELI-D basins 1 and 2 correspond to the S–Cl2 and Cl2–S 'bonds',

Table 3 Numerical analysis of ELI-D topology for **I**.

Atoms and atomic charges: QTAIM / ELIBON		Attribution of ELI-D feature	Basin population q/e$^-$	Bond polarity index p, percentage of prevailing contribution
Re	+1.55 / +3.40	core	57.56	
		penultimate shell	13.83	
		Re–Re disynaptic basin (DB)	0.412	0.01
S	–0.41 / –1.20	core	10.07	
		lone pair (LP)	1.60	
		LP	1.95	
		S–Re DB	1.77	0.56, 78.0% S
		S–Re DB	1.81	0.57, 78.6% S
Cl1	–0.39 / –0.68	core	10.07	
		LP	3.16	
		LP	3.54	
		Cl1–Re DB	0.91	0.58, 78.9% Cl
Cl2	–0.36 / –0.84	core	10.07	
		LP	2.78	
		LP	2.87	
		Cl2–Re DB	1.06	0.64, 82.1% Cl
		Cl2–Re DB	1.06	0.64, 82.2% Cl

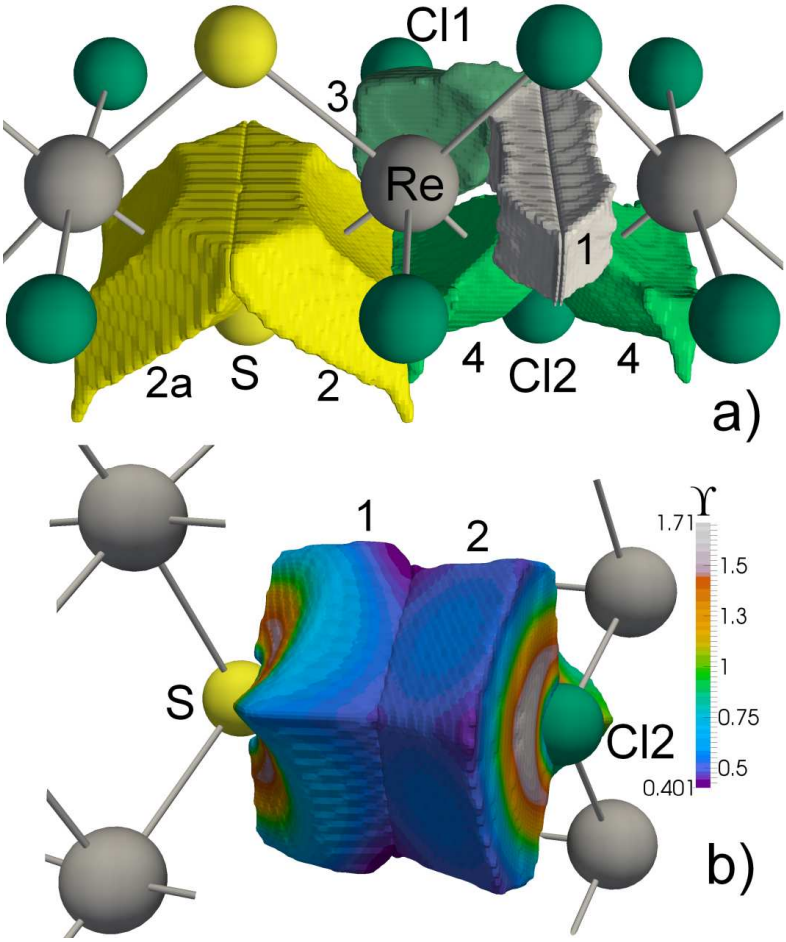

Fig. 8 ELI-D basins for **I**. a) Disynaptic basins and their populations: 1. Re–Re (0.412 *e*); 2, 2a. two S–Re (1.81 *e* and 1.77 *e*); 3. Cl1–Re (0.91 *e*); 4. two Cl2–Re (1.06 *e* each). b) Orientation of two monosynaptic basins showing the interchain interaction: 1. S lone pair (1.60 *e*); 2. Cl2 lone pair (2.78 *e*).

respectively. The ELI-D attractor number 1 is located 0.94 Å from S and 2.78 Å from Cl2, with a high eccentricity (distance perpendicular to the S–Cl2 line) of 0.5 Å. The ELI-D attractor number 2 is located 0.85 Å from Cl2 and 2.78 Å from S, with eccentricity 0.34 Å. Intersection of the ELI-D basin number 1 by the electron density (QTAIM) basins, and integration of the electron density over the resulting intersecting basin, show that S contributes by 99.6 % to the charge in the S–Cl2 ELI-D 'bond' basin number 1. In the case of the Cl2–S 'bond', the same procedure revealed a Cl2 contribution of nearly 100 % to the charge in the Cl2–S ELI-D basin number 2. These ELI-D basins are monosynaptic and describe lone pairs of S and Cl2 with populations of 1.60 and 2.78 *e*, respectively.

Conclusions

The liquid-phase synthesis method allowed obtaining $ReSCl_3$ by interaction between rhenium(VII) oxide and a solution of sulfur in sulfur monochloride at 100°C. The crystal structure of $ReSCl_3$ represents a new structure type of inorganic compounds, which expands the series of one-dimensional chain structures formed by transition metal tetrachlorides. The structure can be described as a packing of distorted edge-shared $Re[Cl_4S_2]$ octahedra forming infinite straight chains along the [010] direction. The Re atoms are arranged in pairs, *i.e.* they form alternatively short and long Re–Re distances within the chains. DOS calculations indicate metallic character. A comparison with the band structures of related compounds suggests that the structure of $ReSCl_3$ with relatively high DOS at E_F, but with weak metal–metal interactions, is on the boundary of stability. Real-space analysis of the chemical bonding with the electron density/electron localizability approach showed that the crystal structure is maintained by covalent polar Re–Cl and Re–S bonds and weak Re–Re non-polar metallic bonds within the chains, and dispersion forces between the chains.

References

[1] D.V. Drobot, B.G. Korshunov, S.L. Kovacheva, *Russ. J. Inorg. Chem.* 17 (1972) 139-140.

[2] Ye.S. Golubyatnikova, V.E. Fedorov, A.P. Mazhara, *Proc. 13th Vses. Nauch. Stud. Konf. Khim.*, Novosibirsk, 1975, p. 11.

[3] I.A. Glukhov, S.B. Davidyants, M.A. Yunusov, N.A. Yemel'yanova, *Russ. J. Inorg. Chem.* 6 (1961) 649-651.

[4] V.G. Tronev, G.A. Bekhtle, S.B. Davidyants, *Tr. Akad. Nauk. Tadzh. SSR* 34 (1958) 105-109.

[5] G.W.A. Fowles, R.J. Hobson, D.A. Rice, K.J. Shanton, *J. Chem. Soc., Chem. Commun.* 14 (1976) 552-553.

[6] N.V. Ulko, V.L. Kolesnichenko, *Z. Neorg. Khim.* 25 (1980) 2565-2567.

[7] V.L. Kolesnichenko, S.P. Sharavskaya, O.G. Yanko, S.V. Volkov, *Russ. J. Inorg. Chem.* 38 (1993) 1011-1015.

[8] S. Rabe, U. Müller, *Z. Anorg. Allg. Chem.* 626 (2000) 830-832.

[9] N.I. Timoshchenko, V.L. Kolesnichenko, S.V. Volkov, Yu.L. Slovokhotov, Yu.T. Struchkov, *Sov. J. Coord. Chem.* 16 (1991) 567-571.

[10] J. Beck, H.K. Müller-Buschbaum, *Z. Anorg. Allg. Chem.* 625 (1999) 1212-1216.

[11] J.-C. Gabriel, K. Boubekeur, P. Batail, *Inorg. Chem.* 32 (1993) 2894-2900.

[12] C. Fischer, S. Fiechter, H. Tributsch, G. Reck, B. Schultz, *Ber. Bunsen-Ges.* 96 (1992) 1652-1658.

[13] *WinXPOW 3.03, Powder Diffraction Software Package*, STOE & Cie GmbH, Darmstadt, Germany, 2010.

[14] *SRM 640b: Silicon Powder 2θ/d-Spacing Standard for X-ray Diffraction*, National Institute of Standards and Technology, U.S. Department of Commerce, Gaithersburg, MD, 1987.

[15] *SRM 676: Alumina Internal Standard for Quantitative Analysis by X-ray Powder Diffraction*, National Institute of Standards and Technology, U.S. Department of Commerce, Gaithersburg, MD, 2005.

[16] A. Altomare, G. Campi, C. Cuocci, L. Eriksson, C. Giacovazzo, A. Moliterni, R. Rizzi, P.-E. Werner, *J. Appl. Crystallogr*. 42 (2009) 768-775.

[17] A. Altomare, C. Cuocci, C. Giacovazzo, A. Moliterni, R. Rizzi, N. Corriero, A. Falcicchio, *J. Appl. Crystallogr*. 46 (2013) 1231-1235.

[18] R.A. Young (Ed.), *The Rietveld Method*, IUCr Monographs on Crystallography, Oxford University Press, New York, Vol. 5, 1993, 298 p.

[19] J. Rodriguez-Carvajal, *Commission on Powder Diffraction (IUCr), Newsletter* 26 (2001) 12-19.

[20] T. Roisnel, J. Rodriguez-Carvajal, *Mater. Sci. Forum* 378-381 (2001) 118-123.

[21] L.M. Gelato, E. Parthé, *J. Appl. Crystallogr*. 20 (1987) 139-143.

[22] K. Brandenburg, *DIAMOND 3.2g, Crystal and Molecular Structure Visualization*, Crystal Impact GbR, Bonn, Germany, 2011.

[23] *The Elk FP-LAPW Code*; http://elk.sourceforge.net/.

[24] J.P. Perdew, A. Ruzsinszky, G.I. Csonka, O.A. Vydrov, G.E. Scuseria, L.A. Constantin, X. Zhou, K. Burke, *Phys. Rev. Lett.* 100 (2008) 136406.

[25] D.D. Koelling, B.N. Harmon, *J. Phys. C: Solid State Phys.* 10, 3107-3114 (1977).

[26] R.F.W. Bader, *Atoms in Molecules, A Quantum Theory*, Clarendon Press, Oxford, 1994.

[27] M. Kohout, *Int. J. Quantum Chem.* 97 (2004) 651-658.
[28] M. Kohout, K. Pernal, F.R. Wagner, Yu. Grin, *Theor. Chem. Acc.* 112 (2004) 453-459.
[29] M. Kohout, *Faraday Discuss.* 135 (2007) 43-54.
[30] M. Kohout, *DGrid*, version 4.6, Radebeul, Germany, 2011.
[31] A.I. Baranov, *Direct Space Topological Partitionings with DGrid and Elk, CECAM Tutorial*, Lausanne, Switzerland, 2011.
[32] K. Momma, F. Izumi, *J. Appl. Crystallogr.* 44 (2011) 1272-1276.
[33] U. Ayachit, *The ParaView Guide: A Parallel Visualization Application*, Kitware, 2015, ISBN 978-1930934306; http://www.paraview.org/.
[34] O.G. Yanko, Z.A. Fokina, V.I. Pekhnyo, S.V. Volkov, *Ukr. Khim. Zh.* 65 (1999) 3-7.
[35] L. Hajba, J. Mink, F.E. Kühn, I.S. Gonçalves, *Inorg. Chim. Acta* 359 (2006) 4741-4756.
[36] V.M. Miskowski, R.F. Dallinger, G.G. Christoph, D.E. Morris, G.H. Spies, W.H. Woodruff, *Inorg. Chem.* 26 (1987) 2127-2132.
[37] S.D. Conradson, A.P. Sattelberger, W.H. Woodruff, *J. Am. Chem. Soc.* 110 (1988) 1309-1311.
[38] W.I.F. David, K. Shankland, L.B. McCusker, Ch. Baerlocher (Eds.), *Structure Determination from Powder Diffraction Data*, IUCr Monographs on Crystallography, Oxford Science Publications, Vol. 13, 2002, 356 p.
[39] P.Yu. Demchenko, R.E. Gladyshevskii, S.V. Volkov, O.G. Yanko, L.B. Kharkova, Z.A. Fokina, A.A. Fokin, *Chem. Commun.* 46 (2010) 4520-4522.
[40] K. Stolze, M. Ruck, *Z. Anorg. Allg. Chem.* 640 (2014) 1559-1563.
[41] D.R. Taylor, J.C. Calabrese, E.M. Larsen, *Inorg. Chem.* 16 (1977) 721-722.
[42] P. Frere, *Ann. Chim. (Paris)* 7 (1962) 85.
[43] H.-G. von Schnering, H. Wöhrle, *Angew. Chem.* 75 (1963) 684.
[44] R.E. McCarley, B.A. Torp, *Inorg. Chem.* 2 (1963) 540-546.
[45] A. Meerschaut, *Acta Crystallogr. E* 62 (2006) i131-i132.
[46] P. Villars, K. Cenzual (Eds.), *Pearson's Crystal Data: Crystal Structure Database for Inorganic Compounds*, Release 2014/15, ASM International, Materials Park, Ohio, USA, 2014.
[47] E.A. Pisarev, D.V. Drobot, I.V. Makarchuk, *Russ. J. Inorg. Chem.* 27 (1982) 10-14.
[48] G. Bergerhoff, K. Brandenburg, in: E. Prince (Ed.), *International Tables for Crystallography*, Vol. C, Ch. 9.4, Kluwer Academic Publishers, Dordrecht, 2004, pp. 778-789.
[49] R.D. Shannon, *Acta Crystallogr. A* 32 (1976) 751-767.
[50] E.V. Johnstone, F. Poineau, P.M. Forster, L. Ma, T. Hartmann, A. Cornelius, D. Antonio, A.P. Sattelberger, K.R. Czerwinski, *Inorg. Chem.* 51 (2012) 8462-8467.
[51] A. Günther, A. Isaeva, A.I. Baranov, M. Ruck, *Chem. Eur. J.* 17 (2011) 6382-6388.
[52] M. Sokolov, H. Imoto, T. Saito, V. Fedorov, *Polyhedron* 17 (1998) 3735-3738.
[53] H.F. Franzen, W. Hönle, H.-G. von Schnering, *Z. Anorg. Allg. Chem.* 497 (1983) 13-20.
[54] P.J. Schmidt, G. Thiele, *Z. Anorg. Allg. Chem.* 625 (1999) 1056-1058.
[55] J. Rijnsdorp, F. Jellinek, *J. Solid State Chem.* 28 (1979) 149-156.
[56] J. Marcoll, A. Rabenau, D. Mootz, H. Wunderlich, *Rev. Chim. Miner.* 11 (1974) 607-615.
[57] P.F. Weck, E. Kim, F. Poineau, E.E. Rodriguez, A.P. Sattelberger, K.R. Czerwinski, *Inorg. Chem.* 48 (2009) 6555-6558.
[58] C.M. Fang, G.A. Wiegers, C. Haas, R.A. de Groot, *J. Phys.: Condens. Matter* 9 (1997) 4411-4424.
[59] S. Tongay, H. Sahin, C. Ko, A. Luce, W. Fan, K. Liu, J. Zhou, Y.-S. Huang, C.-H. Ho, J. Yan, D.F. Ogletree, S. Aloni, J. Ji, S. Li, J. Li, F.M. Peeters, J. Wu, *Nat. Commun.* 5 (2014) 3252 (6 p.).
[60] D. Çakir, H. Sahin, F.M. Peeters, *Phys. Chem. Chem. Phys.* 16 (2014) 16771-16779.
[61] I. Veremchuk, T. Mori, Yu. Prots, W. Schnelle, A. Leithe-Jasper, M. Kohout, Yu. Grin, *J. Solid State Chem.* 181 (2008) 1983-1991.
[62] S. Raub, G. Jansen, *Theor. Chem. Acc.* 106 (2001) 223-232.